 https://doi.org/10.24191/jeesr.v29i1.011

Energy-Efficient PID Control of Agarwood Hydro Distillation using Particle Swarm Optimization

Nurul Nadia Mohammad, Muhammad Imran Hakim Mohd Adnan, Mohd Azri Abdul Aziz, Mohd Hezri Fazalul Rahiman, and Najidah Hambali*

Abstract— **Conventional Proportional Integral Derivative (PID) controllers can provide satisfactory temperature regulation but may exhibit slow transient response and large overshoot when applied to nonlinear and time-varying distillation processes. This study investigates PID tuning for an Agarwood Hydro Distillation Pot using Particle Swarm Optimization (PSO), with a transfer function identified from Pseudo-Random Binary Sequence (PRBS) data. The performance of the Ziegler–Nichols (ZN) controller is compared with PSO-tuned PID controllers using Integral Square Error (ISE), Integral Absolute Error (IAE), Integral Time Square Error (ITSE), and Integral Time Absolute Error (ITAE) as objective functions. The PSO-ISE controller produced the fastest settling time of 1.4926s with 0% overshoot, whereas the other PSO objectives produced settling times of 1.9772–2.9982s. A subsequent fine-tuning of the ZN controller reduced overshoot from 14.773% to 4.73%, but increased the rise time from 1206 s to 2457s and the settling time from 1754.93s to 2361.48s. For energy assessment, the reported quantity is treated as an energy-consumption index because the index is calculated from the error and control signals rather than from a direct electrical power measurement. The PSO-based cases produced an index of 30909.98, while the fine-tuned ZN case produced the lowest value of 25868.83. Thus, PSO provided the best transient response among the tested controllers, while fine-tuning of the ZN controller produced the lowest reported energy consumption index.**

Index Terms — **Agarwood Distillation Pot, PID, PID Tuning Rules, PSO, Energy consumption, water temperature**

I. INTRODUCTION

Agarwood, known for its highly aromatic resin, is a valuable natural product derived from certain tree species of the genus *Aquilaria*. This resin, commonly referred to as "oud," is highly sought after for its use in perfumes, traditional medicine, and religious ceremonies. The production of agarwood oil involves a hydro-distillation process that extracts essential oils from the resinous wood. However, this process is energy-intensive, requiring precise control over temperature and other variables to ensure optimal yield and quality of the extracted oil[1], [2] .

Despite its importance, the hydro-distillation process presents several challenges, particularly in energy efficiency and maintaining consistent product quality. Conventional Proportional Integral Derivative (PID) controllers are commonly employed for controlling temperature and process variables [3]. However, they struggle to handle the nonlinearities and time-varying dynamics inherent to the distillation process [4], [5]. Manual tuning of PID parameters often results in suboptimal performance, leading to energy wastage and reduced yield [6]. Furthermore, the lack of adaptability in traditional control systems exacerbates these issues, especially when dealing with process disturbances or load variations [7], [8], [9]. Recent advancements in optimization techniques have expanded the available approaches for PID parameter tuning. A recent review reported the use of Genetic Algorithms (GA), Particle Swarm Optimization (PSO), Differential Evolution (DE), Artificial Bee Colony (ABC), Grey Wolf Optimization (GWO), and other nature-inspired methods for PID tuning, highlighting that their effectiveness depends on the application and objective function [10]. Recent studies also show that different optimizers can exhibit different strengths: GA and PSO, for example, can provide different convergence and robustness characteristics under nonlinear process disturbances [11], while improved PSO variants have been reported to reduce overshoot, steady-state error, and response time relative to conventional PID and PSO-PID implementations [12]. Multi-objective methods based on other metaheuristics have likewise been investigated to balance several error and transient-performance criteria simultaneously [13]. Therefore, the present study does not assume that PSO is universally superior; instead, it evaluates PSO for the specific dynamics and performance objectives of the Agarwood Hydro Distillation Pot.

This manuscript is submitted on April 23, 2026, revised on September 15, 2026, accepted on October 19, 2026, and published on October 31, 2026.

Nurul Nadia Mohammad is from Faculty of Electrical Engineering, Universiti Teknologi MARA, Cawangan Terengganu, Kampus Dungun, Terengganu, Malaysia

Muhammad Imran Hakim Mohd Adnan, Mohd Azri Abdul Aziz, Mohd Hezri Fazalul Rahiman and Najidah Hambali are from Faculty of Electrical Engineering, Universiti Teknologi MARA, Shah Alam, Selangor, Malaysia.

*Corresponding author
Email address: najidah@uitm.edu.my

1985-5389/© 2026 The Authors. Published by UiTM Press. This is an open access article under the CC BY-NC-ND license (http://creativecommons.org/licenses/by-nc-nd/4.0/).

The Ziegler-Nichols (ZN) tuning method, a widely used approach for PID parameter tuning, relies on the process reaction curve or ultimate gain and period to determine the proportional, integral, and derivative gains. While the ZN method provides a straightforward and systematic way of obtaining initial tuning parameters, it is often insufficient for nonlinear and time-varying systems like the agarwood hydro-distillation process [14], [15]. This can result in suboptimal controller performance with longer settling times, higher overshoots, and reduced energy efficiency [16]. The integration of advanced optimization techniques like PSO can address these limitations by dynamically adjusting the PID parameters to achieve better control performance.

The primary objective of this study is to evaluate PSO-based PID tuning for the Agarwood Hydro Distillation Pot while explicitly examining the trade-off between transient performance and the energy-consumption index. The specific goals are to estimate the system transfer function using PRBS signals, compare Ziegler–Nichols-tuned PID with PSO-tuned PID using four objective functions, evaluate the effect of subsequent ZN fine-tuning, and clarify the relationship between controller performance and the reported energy-consumption index. The conclusions are limited to the tested model, operating conditions, and objective functions.

The remaining of this paper is structured as follows: Section II reviews the experimental setup and Section III describes system identification, PID design, PSO implementation, fine-tuning, and the energy-consumption index. Section IV presents the results, including transfer-function selection, PSO tuning, transient-response comparison, fine-tuning, energy assessment, robustness tests, and comparison with recent optimization approaches. Section V concludes the study and identifies directions for future research.

II. Experimental Design

This project aims to develop an optimized PID controller for the Agarwood Hydro Distillation Pot using PSO, focusing on enhancing energy efficiency while maintaining precise temperature control for quality essential oil extraction [17]. The experimental design involves system identification, transfer function modeling, and PSO-based controller tuning, with comparisons to conventional PID controllers. The system, shown in Fig. 1, consists of a stainless-steel tank equipped with a heating element, a condenser made of copper, and a temperature monitoring device such as a Resistance Temperature Detector (RTD). Similar designs have proven effective in controlling steam temperature in distillation systems.[18, 19]. critical moment where the temperature increased significantly due to pressure buildup within the system.

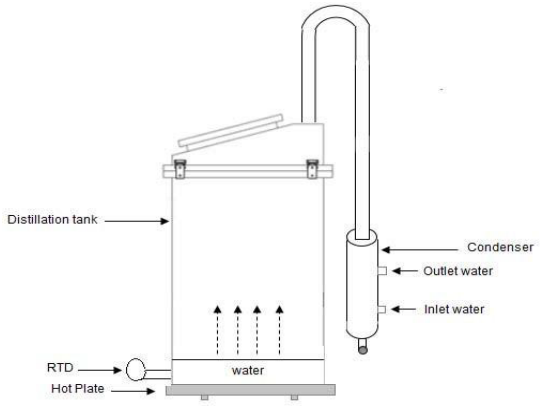


Fig. 1. Hydro distillation process.

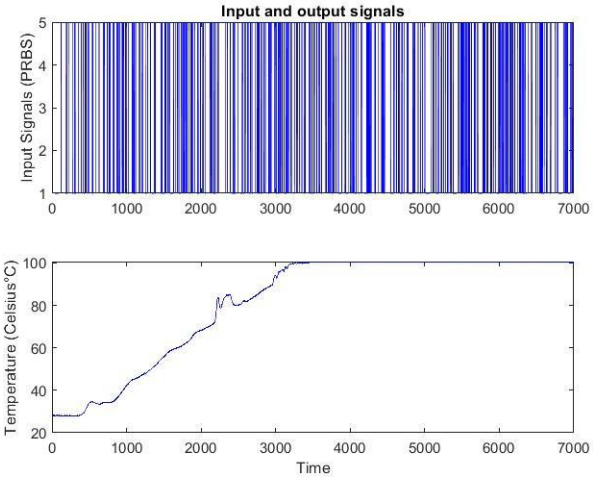


Fig. 2(a). Open-loop temperature response **(b).** 5V step input signal.

In this study, an open-loop experiment was conducted to analyze the system's temperature dynamics. The results, illustrated in Fig. 2 (a) and Figure 2 (b), show the open-loop temperature response and the system's reaction to a 5V step input signal, respectively. The response highlights a critical moment where the temperature increased significantly due to pressure buildup within the system.

III. Methodology

Accurate estimation of transfer functions is essential for the design of effective control strategies. The proposed tangent method provides a precise framework for identifying system parameters, even in complex and nonlinear systems. Once a reliable transfer function is obtained, a PID controller can be implemented, leveraging its simplicity, effectiveness, and ease of implementation to regulate system outputs and correct performance errors through proportional, integral, and derivative actions.

A. Transfer Function Estimation

The first step involves estimating the system's transfer function using data from the open-loop response. The Pseudo Random Binary Signal (PRBS) is employed as the

perturbation input to capture the system's dynamic behavior. The MATLAB "System Identification" toolbox in Fig. 3 is used to analyze the data and identify the best-fit model based on metrics such as Mean Squared Error (MSE), Final Prediction Error and the R-squared value. This transfer function forms the basis for the controller design. The formulas are provided in equation (1), (2), and (3).

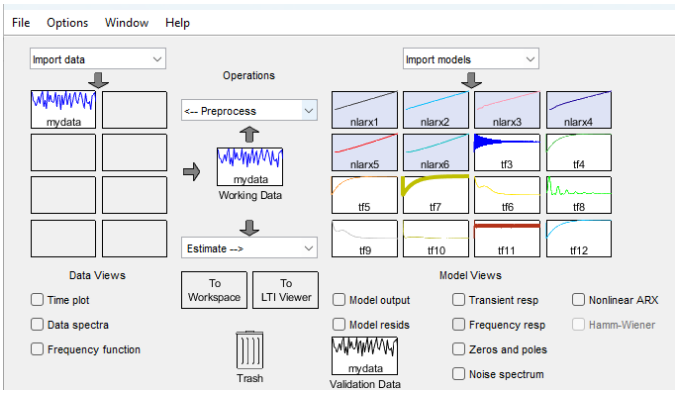


Fig. 3: System Identification.

R-squared, or the coefficient of determination, is used to measure how effectively the variability in the data is explained by the model, with values closer to 1 indicating a stronger fit [20]. A high R-squared value, typically above 0.75, is considered an indication that most of the data's variation is captured and the underlying system is accurately represented [5]. Mean Square Error is calculated as the average squared difference between predicted and actual values, where smaller values are seen as evidence of higher accuracy and better alignment between the model and the data. Final Prediction Error is employed to balance model accuracy and complexity, ensuring good generalization to new data. When R-squared exceeds 0.75 and the Mean Square Error is reduced below 5.0, or ideally below 1.0, the model is regarded as having excellent accuracy and alignment with the system being represented [21].

The R-Squared formula as mentioned in equation (1) was applied to evaluate the FIT estimation, providing a measure of how well the model aligns with the observed data across the specified intervals.

$$R^2 = 1 - \frac{\sum_{i=1}^{n}(y_i - \hat{y}_i)^2}{\sum_{i=1}^{n}(y_i - \bar{y}_i)^2} \quad (1)$$

The Mean Square Error (MSE) was computed to evaluate the model's accuracy by measuring the average squared difference between the predicted and observed values. The formula for MSE will be referred to in equation (2). A lower MSE indicates that the model's predictions are more closely aligned with the actual data, reflecting higher accuracy and reliability [22].

$$MSE = \frac{\sum_{i=1}^{n}(e_i)^2}{n} = \frac{\sum_{i=1}^{n}(y_i - \hat{y}_i)^2}{n} \quad (2)$$

The Final Prediction Error (FPE) was utilized to evaluate the model's ability to predict new, unseen data, considering both the model's accuracy and its complexity. The formula for FPE will be referenced in equation (3). A smaller FPE value suggests better generalization of the model, indicating that it avoids overfitting while still providing accurate predictions.

$$FPE = det\left[\frac{1}{N}\sum_{1}^{N}\left((t,\theta_N)\right)^T\right]\left[\frac{1+\frac{d}{N}}{1-\frac{d}{N}}\right] \quad (3)$$

B. PID Controller

The PID controller is used to regulate a process by adjusting the control input based on three components: proportional (Kp), integral (Ti), and derivative (Td). The proportional component (Kp) adjusts the output in proportion to the current error, providing immediate correction. The integral component (Ti) addresses the accumulation of past errors, eliminating steady-state error over time. The derivative component (Td) predicts future errors by considering the rate of change in the error, improving system stability [23]. The tuning of Kp, Ti, and Td is crucial for achieving optimal performance. In this study, the process reaction curve, as shown in Figure 4, is utilized to analyze the system's dynamics and aid in the estimation of key parameters required for tuning the PID controller. The study focuses on well-known tuning approaches such as ZN.

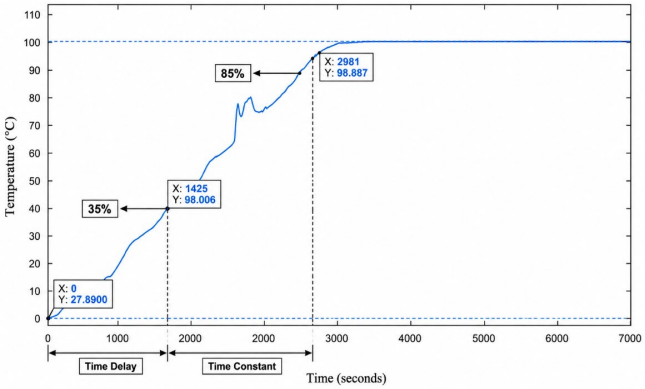


Fig. 4: Process Reaction Curve.

It was suggested that the times t1 and t2 be determined from the step response curve, corresponding to the response times of 35.3% and 85.3%, respectively. The time delay, θ and time constant, τ are then calculated using the corresponding equations (4), (5) and (6).

$$Gain, K = \frac{output\ \Delta y}{input\ \Delta x} \quad (4)$$

$$Time\ Constant, \tau = 0.67(t2 - t1) \quad (5)$$

$$Time\ Delay, \theta = 1.3\,(t_1 - t_{step}) - 0.29(t_2 - t_{step}) \quad (6)$$

The formula for determining these parameters is provided in Table 1, while the calculated results are presented in Table 1.

TABLE I. FORMULA FOR PID TUNING

PID Tuning	Proportional Gain, Kp	Integral Time constant, Ti	Derivative Time Constant, Td
ZN	$(\mathbf{1.2}/\boldsymbol{K})\,(\boldsymbol{\tau}/\boldsymbol{\theta})$	$2\boldsymbol{\theta}$	$0.5\boldsymbol{\theta}$

$$\mu(t) = K_P\left(e(t) + \frac{1}{T_i}\int_0^t e(t) + T_d\frac{de(t)}{dt}\right) \quad (7)$$

C. Particle Swarm Optimization (PSO)

Once the system model is identified, the next step is to optimize the PID controller parameters using the PSO algorithm. PSO is a computational optimization technique inspired by the social behavior of birds and fish[24], [25], [26]. It is used to find the optimal solution to a problem by iteratively improving a candidate solution set called particles. Each particle represents a potential solution and moves through the search space based on its velocity, which is influenced by its own best position and the best position found by the swarm. The algorithm balances exploration and exploitation using parameters such as inertia weight, cognitive coefficient, and social coefficient. PSO is widely used for optimizing complex systems due to its simplicity, flexibility, and ability to handle nonlinear and multi-dimensional problems efficiently [2], [27], [28]. The optimized set of PID parameters is derived, aiming to enhance the system's performance based on the equations (7) and (8).

$$v_{id}^{n+1} = wv_{id}^{n} + c_1 rand_1()(P_{id}^{n} - x_{id}^{n}) + c_2 rand_2()(P_{gd}^{n} - x_{id}^{n}) \quad (7)$$

$$x_{id}^{n+1} = x_{id}^{n} + v_{id}^{n+1} \quad (8)$$

The n denotes the number of iterations, rand1 and rand2 are random values within the range of (0,1), w is the inertia weight coefficient, c_1 and c_2 are the learning factors, and P_{id}^{n} corresponds to the optimal position for each generation.

In the implementation, each particle represents a candidate PID parameter vector, x = [Kp, Ti, Td]. For each particle, these three parameters are assigned to the PID controller connected to the identified third-order, two-zero plant model, and the closed-loop response is simulated for the 85 °C setpoint. The tracking error e(t) = r(t) − y(t) is then used to calculate the selected objective function. Four separate PSO runs are performed, one for each criterion: ISE, IAE, ITSE, and ITAE. Thus, the optimization is repeated with a different cost function rather than combining all four indices into one objective. The resulting objective value is used to compare the candidate with the particle's personal-best solution and the swarm's global-best solution. Particle velocities and positions are updated using the inertia, cognitive, and social terms in Equations (7) and (8), and this evaluation–update cycle continues until the stopping condition is reached. The best parameter vector from each run is then used in the corresponding closed-loop simulation, and rise time, peak time, overshoot, and settling time are compared in Table VI.

For reproducibility, the population size, numerical bounds imposed on Kp, Ti, and Td, the initialisation procedure, the specific values or schedules for the inertia weight and learning coefficients, the maximum iteration count, and the stopping tolerance should be reported alongside the equations. These implementation settings are not specified numerically in the current study; therefore, the reported results should be interpreted as the outcomes of the implemented simulation rather than as a fully reproducible specification of the PSO search. The four objective functions are defined in Equations (9)–(12), and the parameter values obtained for each run are reported in Table V.

After the controllers have been enhanced through optimization, both PID types are placed in the system to evaluate their performance. The system is initially tested with a PID controller, whose parameters have been manually adjusted, to monitor performance metrics such as power consumption and extracted oil quality. Subsequently, the PID-PSO controller is applied to the system, and each performance metric is measured for evaluation. These evaluation methods are used to assess the effectiveness of different control approaches and parameter values. The best configuration is selected by examining performance metrics that indicate faster response time, steady system behavior, and lower error rates. In this study, PSO is applied to tune PID parameters. The performance of each candidate solution is evaluated using common objective functions such as Integral Absolute Error (IAE), Integral Square Error (ISE), Integral Time Square Error (ITSE), and Integral Time Absolute Error (ITAE). The equations below are used to determine the errors associated with each of these indices.

$$ISE = \int e^2 dt \quad (9)$$

$$IAE = \int |e| dt \quad (10)$$

$$ITSE = \int te^2 dt \quad (11)$$

$$ITAE = \int t|e| dt \quad (12)$$

The variable e(t) represents the gap between the target input r(t) and the real output y(t). The PID controller takes e(t) as input to create both integral and derivative measurements of this error signal. Equation (13) shows how error signals serve as a tool for PID controller adjustment.

$$\mu(t) = K_P\left(e(t) + \frac{1}{T_i}\int_0^t e(t) + T_d\frac{de(t)}{dt}\right) \quad (13)$$

The equation u(t) represents the PID controller, incorporating three key components, proportional, integral, and derivative terms. The proportional term, based on Kp and e(t), provides an immediate response to the current error. The integral term,

involving Ti accumulates past errors to correct steady-state errors and ensure the system reaches its desired setpoint. The derivative term, defined by Td, addresses the rate of change of error, helping to predict future behavior and reduce oscillations. Together, these terms adjust u(t), improving the system's performance by reducing error, enhancing stability, and minimizing steady-state deviations.

$$J = \int_0^{\infty} w_1|e(t)| + w_2u^2(t))dt + w_3t_u \quad (14)$$

$$If ey(t) < 0, J = \int_0^{\infty}\big(w_1|e(t)| + w_2u(t)\big)dt + w_4|ey(t)| + w_3t_u \quad (15)$$

$$ey(t) = y(t) - y(t-1) \quad (16)$$

The equations (14) and (15) represent cost functions for control system optimization. In equation (14), the cost function J includes the weighted error $w_1|e(t)|$, the control effort $w_2u^2(t)$, and w_3t_u, which accounts for time-related factors. In equation (14), an additional term $w_4|ey(t)|$ is introduced when the error e(t) is negative, penalizing rapid changes in the system's output, where ey(t)=y(t)-y(t-1). The weights w_1, w_2, w_3, and w_4 are used to balance error, control effort, and system stability, with the goal of minimizing the cost function by optimizing the system's performance.

D. Fine Tuning

The fine-tuning stage was performed after the initial Ziegler–Nichols tuning and should be distinguished from the PSO optimization. The purpose of fine-tuning was to improve stability by adjusting the ZN integral and derivative time constants. The proportional gain was kept constant, while Ti and Td were increased as shown in Table VII. This adjustment reduced overshoot, but it also increased rise time, peak time, and settling time. Therefore, fine-tuning is interpreted here as an empirical stability adjustment of the ZN controller rather than as a competing metaheuristic optimization algorithm.

TABLE II . FORMULA FOR PID FINE TUNING

PID Tuning	Proportional Gain, Kp	Integral Time constant, Ti	Derivative Time Constant, Td
ZN	Kp	2 Ti	0.25 Td

E. Evaluation of energy consumption

In this section, the energy-related result is evaluated using the energy consumption index defined in Equation (16). The index is calculated from the error signal and control signal, as illustrated in Fig. 5, and is therefore reported as an index rather than as directly measured electrical energy. Unless a calibrated power measurement is introduced, the numerical values should not be interpreted as physical electrical energy in joules or power in watts. Lower values indicate a lower accumulated value of the defined index under the same simulation conditions.

$$J = \sum_{t=0}^{on} \| e(t) \|^2 + \sum_{t=0}^{\infty} \| e(u) \|^2 \quad (16)$$

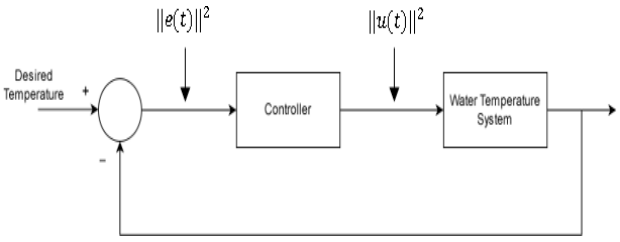


Fig. 5: Evaluation of Energy Consumption.

IV. RESULT AND DISCUSSION

In this part, the result demonstrates the evaluation of transfer function selection, PID tuning value and PID performance comparison.

A. Transfer Function Estimation

From Table III, the third-order, second-zero model was selected for subsequent controller design because it provided a strong fit of 92.39% with MSE = 3.844 and FPE = 3.854. Although the five-pole, two-zero model produced a slightly higher fit of 93.09%, the selected third-order model provides a simpler representation with a comparatively low MSE and FPE. The selection was therefore based on the combined fit, prediction error, and model complexity rather than on fit percentage alone.

The selected transfer function obtained from the system-identification analysis was subsequently implemented in the transfer-function block together with the PID controller for the closed-loop simulations.

$$G(s) = \frac{0.02024S^2 + 1.244x10^5S + 7.032x10^8}{s^3 + 0.002292s^2 + 4.329x10^6s + 1.939x10^9} \quad (16)$$

Table III presents the model-selection results, while Table VI presents the PID parameters obtained from the PSO running. The PSO tuning was evaluated separately using ISE, IAE, ITSE, and ITAE, allowing the effect of the selected objective function on the controller gains and transient response to be examined. The results show that the number of poles and zeros significantly affects the model identification accuracy. In general, a good model should have a high R^2 value and low MSE and FPE values, indicating that the model fits the experimental data well while minimizing prediction errors. The model with 3 poles and 2 zeros achieves the best performance, with R^2 = 92.3 %, MSE = 3.844, and FPE = 3.854. This indicates that this configuration provides the best balance between model accuracy and prediction error among the tested

configurations. Although increasing the number of poles and zeros can improve model flexibility, it does not necessarily improve accuracy, as demonstrated by the inconsistent results for models with 4 and 5 poles. Overall, the 3-pole, 2-zero model is the most suitable model among those evaluated based on the three performance indicators.

TABLE III. FIT, MSE, AND FPE RESULT OF POLES AND ZERO

No. of pole(s)	No. of zero(s)	R^2 (%)	MSE	FPE
1	0	80.91	24.16	24.18
	1	80.94	24.09	24.12
2	0	-8.996	787.8	788.923
	1	15.7	471.2	472
	2	56.72	124.2	124.4
3	0	47.19	185	185.3
	1	69.75	60.81	60.67
	2*	**92.39***	**3.844***	**3.854***
	3	92.14	4.097	4.109
4	0	75.65	39.31	39.41
	1	62.12	95.15	95.43
	2	-33.82	1188	1191
	3	85.05	14.82	14.87
	4	6.606	578.4	580.6
5	**0**	34.28	286.4	287.3
	1	33.2	295.9	296.9
	2	93.09	3.164	3.176
	3	13.96	490.9	492.9
	4	91.17	5.172	5.194
	5	91.73	4.537	4.558

*the best result

B. PID Control Parameter

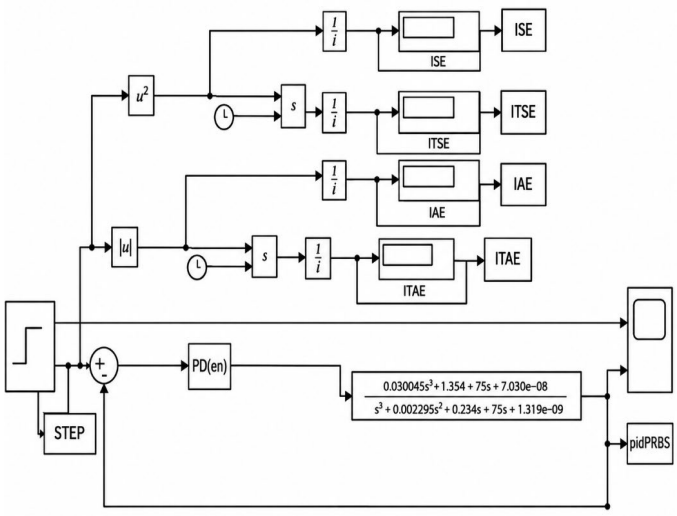


Fig. 6: PSO-PID Block Diagram.

Fig. 6 presents the PSO-PID implementation used for tuning. The identified plant is connected to the PID controller, while parallel error-calculation paths evaluate ISE, IAE, ITSE, and ITAE. Each objective function is used to evaluate candidate PID parameters, and the resulting optimum parameter set is reported in Table IV. Table VI presents the PID parameters obtained from the PSO running. The PSO tuning was evaluated separately using ISE, IAE, ITSE, and ITAE, allowing the effect of the selected objective function on the controller gains and transient response to be examined.

TABLE IV. FIT, MSE, AND FPE RESULT OF POLES AND ZERO

Type of error	Value
ISE	0.00133
IAE	0.17645
ITSE	0.01029
ITAE	0.07217

Table IV lists the numerical values of the four objective functions used during the PSO tuning procedure. These values define the performance criteria used to obtain the PID parameters reported in Table V. Table IV presents the performance evaluation of the developed control system using four performance indices: Integral Square Error (ISE), Integral Absolute Error (IAE), Integral Time Square Error (ITSE), and Integral Time Absolute Error (ITAE). The results show that ISE achieves the lowest value of 0.00133, followed by ITSE at 0.01029, ITAE at 0.07217, and IAE at 0.17645. These indices evaluate the control error from different perspectives, with ISE and ITSE penalising larger errors more heavily, while ITSE and ITAE additionally account for the duration of the error. Overall, the low ISE value indicates that the squared control error is small, while the ITSE and ITAE values provide further insight into error persistence over time. However, since the indices use different mathematical formulations, their numerical values should not be compared directly to rank controller performance. Instead, they should be used collectively to assess the controller's error magnitude and response over time.

Table V presents the PID controller parameters obtained using the different tuning approaches. Ziegler–Nichols is used as the classical baseline, while PSO is used to tune Kp, Ti, and Td separately for ISE, IAE, ITSE, and ITAE. The resulting gains differ substantially according to the selected objective function, confirming that the optimization criterion directly influences controller behavior. In particular, the ISE solution produces the fastest transient response in Table VI, while the IAE, ITSE, and ITAE solutions provide alternative compromises among rise time, overshoot, and settling time. The results support the use of PSO as an effective tuning method for this particular identified model, but they do not establish that PSO is universally superior to other optimization techniques.

TABLE V. VALUE OF PID TUNED USING PSO

PID Tuning Rule		Proportional Gain, Kp	Integral Time, Ti	Derivative Time, Td
Ziegler-Nichols		0.0837	2013.62	503.405
PSO	ISE	562.496	3.113	534.88
	IAE	363.710	850.431	136.86
	ITSE	343.759	310.593	123.63
	ITAE	932.413	895.343	295.74

C. PID Control Performance

The target temperature of 85°C was set to evaluate the performance of the controllers using the estimated transfer functions, as this temperature is considered optimal for maintaining the quality of the oil [14], [28]. The controllers' performance was assessed based on key metrics such as rise time, settling time, peak time and percent overshoot, with the results summarized in Table 6.

Table VI. compares the performance of PID controllers using various tuning methods, including ZN and PID-PSO techniques. The ZN method results in a rise time of 1206 seconds, a peak time of 3299.78 seconds, a percent overshoot of 14.773%, and a settling time of 1754.93 seconds. While ZN has a relatively high peak time, it is often chosen for its simplicity and effectiveness in certain systems, though it sacrifices fast stabilization for better long-term performance. When using PSO to tune PID controllers, various performance indices such as Integral Absolute Error (IAE), Integral Square Error (ISE), Integral Time Square Error (ITSE), and Integral Time Absolute Error (ITAE) are used as objective functions. These indices influence the tuning results and lead to varied control performance outcomes. The ISE method from PSO is selected due to its lowest settling time of 1.4926 seconds, despite its higher peak time. This is because ISE optimizes the controller's parameters by focusing on minimizing the overall error, resulting in faster stabilization and minimal overshoot, which makes it more effective for achieving quick response and accuracy. Fig. 8 illustrates the performance comparison between ZN and PSO tuning methods.

D. Comparison with Recent Optimization Techniques

Recent literature indicates that the relative performance of optimization algorithms depends strongly on the plant, objective function, and disturbance scenario. Patil et al. [10] reviewed GA, PSO, DE, ABC, GWO, and other nature-inspired approaches and emphasized that different methods offer different strengths for PID tuning. Ajlouni et al. [11] compared GA- and PSO-based approaches for nonlinear CSTR processes and reported different convergence and robustness characteristics under disturbances, illustrating that neither algorithm is universally dominant. Hu et al. [12] showed that an improved PSO can outperform conventional PID and conventional PSO-PID for a marine dual-fuel engine, particularly in overshoot, steady-state error, and response time. Yang et al. [13] further demonstrated the use of a multi-objective marine predator algorithm with a whale-optimization component to balance several transient-performance objectives. Compared with these studies, the present work uses standard PSO with four conventional error indices and focuses on an agarwood hydro-distillation temperature model. The present results show that PSO-ISE gives the best transient response among the tested controllers, while the separately fine-tuned ZN controller gives the lowest energy-consumption index. This distinction is important: the current study demonstrates application-specific performance rather than universal superiority of PSO.

TABLE VI. PID PERFORMANCE'S

PID Tuning Rule		Rise Time (s)	Peak Time (s)	Overshoot (%)	Settling Time (s)
Ziegler-Nichols		1206	3299.78	14.773	1754.93
PSO	ISE	0.0016	1.07	0	1.4926
	IAE	0.3251	1.15	8.5939	1.9772
	ITSE	0.3974	1.64	5.6055	2.9982
	ITAE	0.4053	1.31	2.4245	1.7641

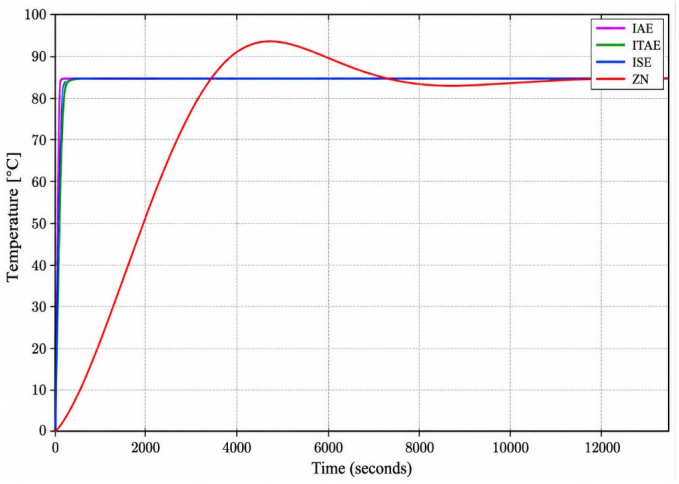


Fig. 8: Comparison plot between PSO and Ziegler-Nichols.

E. Fine Tuning Performance

As shown in Table VII, the proportional gain, Kp remained constant, but the integral time constant Ti and derivative time constant, Td were significantly increased. The integral time constant doubled from 2013.62 to 4027.24, allowing the controller to address steady-state errors more effectively, while

the derivative time constant increased from 503.405 to 1006.81, improving the predictive response and reducing system overshoot. Table VIII highlights the performance improvements achieved through fine-tuning. While the rise time increased from 1206 seconds to 2457 seconds and the peak time rise from 3299.78 seconds to 6951.5 seconds, the overshoot was significantly reduced from 14.773 % to 4.73 %. This demonstrates that fine-tuning prioritized system stability by minimizing oscillations. However, the settling time also increased from 1754.93 seconds to 2361.48 seconds, indicating a trade-off between faster response and improved precision. The fine-tuning process as in Fig. 9, significantly impacted the performance of the PID controller by adjusting its parameters to enhance system stability and dynamic response. These changes reflect a shift towards a more stable and energy-efficient system.

The comparison should not be interpreted as evidence that fine-tuning is generally better than PSO, or that PSO is superior on every criterion. The PSO-ISE controller achieved the shortest settling time (1.4926 s) and zero overshoot among the tested PSO cases, whereas fine-tuning the ZN controller reduced overshoot from 14.773% to 4.73% but increased rise time from 1206 s to 2457 s and settling time from 1754.93 s to 2361.48 s. These outcomes reflect different priorities: PSO optimised tracking-error indices, while the manual fine-tuning adjusted the ZN integral and derivative time constants to reduce overshoot. In addition, the reported energy-consumption index is derived from error and control signals, not from direct electrical power measurements. The fine-tuned ZN case therefore has the lowest value of this defined index (25868.83), but this result alone does not establish lower physical energy use or overall controller superiority. A fairer overall comparison would require applying the same explicitly defined objective function and constraints to all methods, together with experimental power measurements if energy efficiency is claimed.

TABLE VII. VALUE FOR PID PARAMETER

PID Tuning	Proportional Gain, Kp	Integral Time constant, Ti	Derivative Time Constant, Td
Ziegler-Nichols	0.0837	2013.62	503.405
Fine Tuning	0.0837	4027.24	1006.81

TABLE VIII. COMPARISON PARAMETER BEFORE AND AFTER FINED TUNING

PID Tuning Rule	Rise Time (s)	Peak Time (s)	% Overshoot (%OS)	Settling Time (s)
Before Fine Tuning	1206	3299.78	14.773	1754.93
After Fine Tuning	2457	6951.5	4.73	2361.48

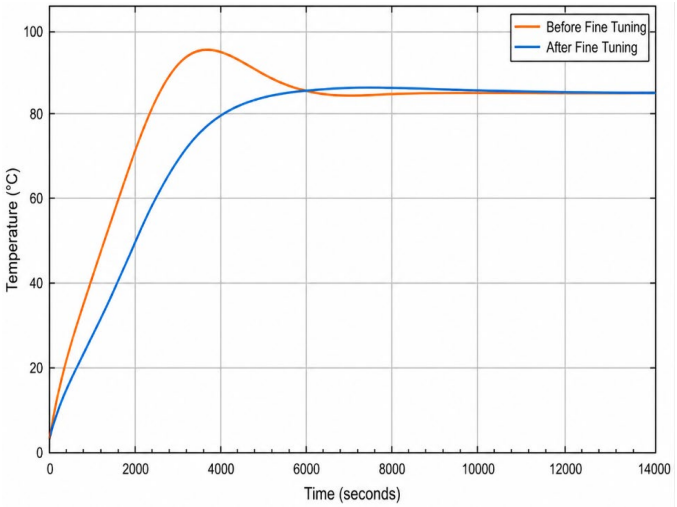


Fig. 9: Comparison plot before and after fine tuning.

F. Energy Consumption and Robustness Test

Table IX and Fig. 10 present the obtained energy consumption values for the Ziegler–Nichols (ZN) tuning method before and after fine-tuning, as well as the results obtained using Particle Swarm Optimization (PSO) based on four performance indices which is ISE, IAE, ITSE, and ITAE. The results show that fine-tuning reduces the energy consumption from 30,509.89 to 25,868.83, demonstrating an improvement in energy efficiency compared with the original ZN controller. In contrast, all four PSO-based tuning methods produce the same energy consumption value of 30,909.98. This indicates that, based on the reported results, the PSO-based methods do not demonstrate a reduction in energy consumption relative to the original ZN controller. Therefore, fine-tuning the ZN controller appears to be more effective in reducing energy consumption under the evaluated conditions. On the hand, this may be attributed to the fact that PSO focuses on optimising the controller's performance according to the selected error-based objective function but does not explicitly consider the energy consumption index as an optimisation objective.

TABLE IX. OBTAINED VALUE OF ENERGY CONSUMPTION

Tuning Method		Energy Consumption
Ziegler-Nichols	Before Fine Tuning	30509.89
	After Fine Tuning	25868.83
PSO	ISE	30909.98
	IAE	30909.98
	ITSE	30909.98
	ITAE	30909.98

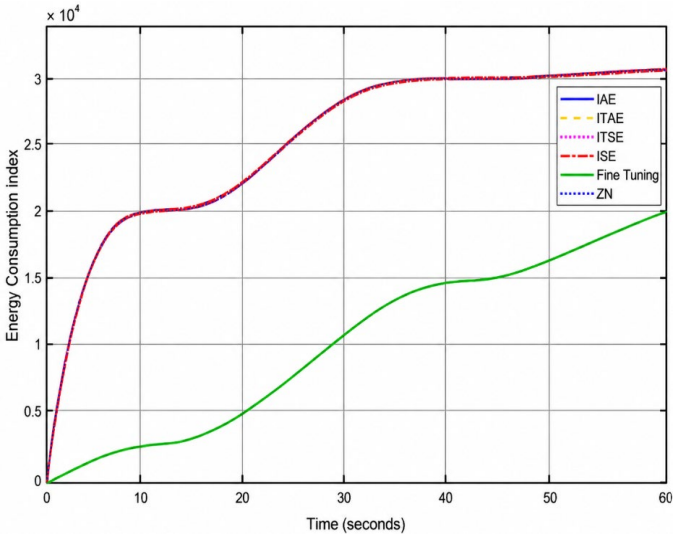


Fig.10: Comparison of Energy Consumption.

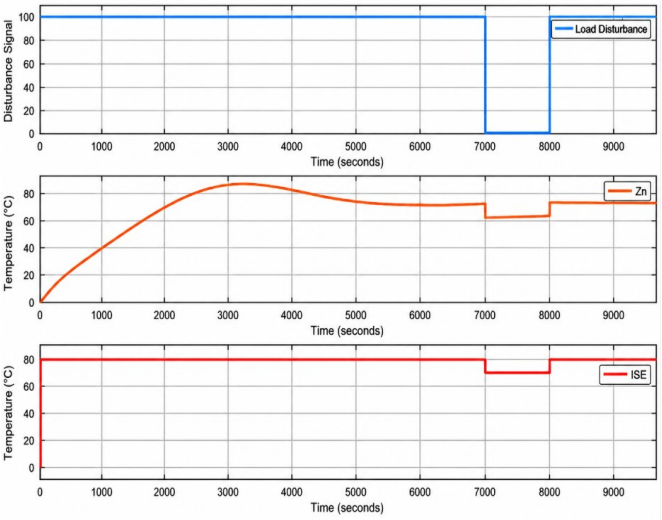


Fig. 11: Comparison of Energy Consumption.

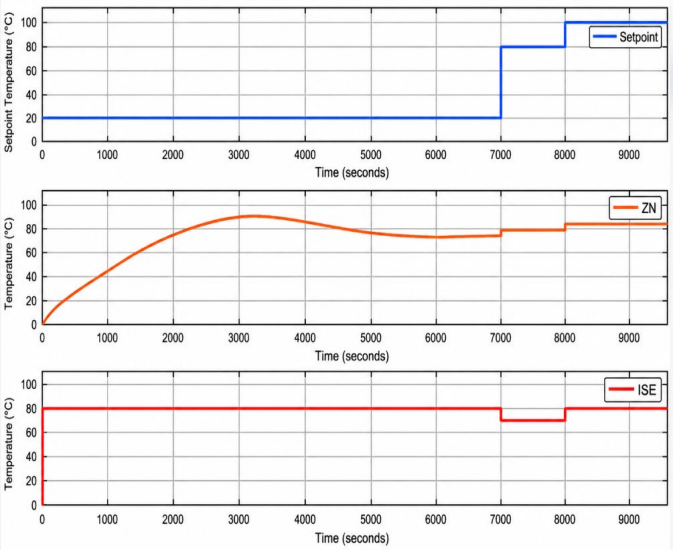


Fig. 12: Comparison of Energy Consumption.

Fig. 11 compares the response of the ZN and PSO-ISE controllers under load disturbances applied at 7000s and 8000s after the system reached a stable state. The ZN controller exhibits larger deviations and a longer recovery period, whereas the PSO-ISE controller provides a smoother response and smaller deviations from the setpoint. Fig. 12 shows the corresponding step-change test. The ZN controller responds more aggressively and exhibits larger overshoot, while the PSO-ISE controller provides a slower but more stable adjustment. These results support the conclusion that PSO-ISE offers better disturbance rejection and transient stability for the tested conditions, without implying that it is superior for all possible operating conditions.

V. Conclusion

This study evaluated Ziegler–Nichols, PSO-tuned, and fine-tuned PID controllers for temperature control of an Agarwood Hydro Distillation Pot. The third-order, second-zero transfer-function model was selected with a 92.39 % fit, MSE of 3.844, and FPE of 3.854. Among the PSO cases, the ISE objective produced the best transient response, with a settling time of 1.4926 s and 0% overshoot, while the other PSO objectives produced settling times between 1.7641s and 2.9982s. The ZN controller was slower and exhibited 14.773 % overshoot. Fine-tuning of the ZN controller reduced overshoot to 4.73 %, but increased rise time and settling time, demonstrating a clear stability-versus-speed trade-off. For the energy assessment, the reported quantity is treated as an energy-consumption index derived from the error and control signals. The PSO cases produced an index of 30909.98, whereas fine-tuning reduced the ZN index to 25868.83, the lowest among the tested configurations. Therefore, the results do not support a claim that PSO is simultaneously the best method for transient performance and energy consumption. Instead, PSO-ISE is the best-performing approach for the tested transient-response criteria, while fine-tuned ZN provides the lowest reported energy consumption index. This application specific distinction strengthens the interpretation of the results and provides a more balanced basis for comparison with other optimization methods.

Fine-tuning improved the stability-related response by reducing overshoot, but it did not improve all transient metrics and should not be classified as superior to PSO overall. The results highlight the importance of selecting an objective function that reflects the intended control priority.

Future research could focus on extending the comparison to other optimization techniques such as Genetic Algorithm, Differential Evolution, Artificial Bee Colony, Grey Wolf Optimization, and hybrid PSO-based methods. In particular, a multi-objective optimization framework that simultaneously

minimizes tracking error, overshoot, settling time, and the energy-consumption index would provide a more direct assessment of energy-efficient control. Real-time adaptive tuning and experimental validation under varying water volume, heating load, and process disturbances could further establish the robustness of the controller.

ACKNOWLEDGMENT

The authors would like to thank to the Faculty of Electrical Engineering, Universiti Teknologi MARA Shah Alam Selangor for support and facilities provided for this research.

REFERENCES

[1] Mehdi Nasri, Hossein Nezamabadi-pour, and Malihe Maghfoori, "A PSO-Based Optimum Design of PID Controller for a Linear Brushless DC Motor," pp. 211–215, 2007.

[2] Adnan Mukhtar, Vijay Kumar Tayal, and HP. Singh, "PSO Optimized PID Controller Design for the Process Liquid Level Control," in *2019 3rd International Conference on Recent Developments in Control, Automation & Power Engineering (RDCAPE)*, 2019.

[3] E. A. Aner, M. I. Awad, and O. M. Shehata, "Performance evaluation of PSO-PID and PSO-FLC for continuum robot's developed modeling and control," *Sci Rep*, vol. 14, no. 1, Dec. 2024, doi: 10.1038/s41598-023-50551-0.

[4] S. Ben Abdi, A. Debilou, A. Guergazi, Y. Samsar, and M. Labed, "Speed Control of BLDC Quadrotor Motor Using an ANN Trained with PID Controller Data Optimized by PSO Algorithm," in *Proceedings - 8th IEEE International Conference on Image and Signal Processing and their Applications, ISPA 2024*, Institute of Electrical and Electronics Engineers Inc., 2024. doi: 10.1109/ISPA59904.2024.10536817.

[5] L. A. Casaverde, R. H. Risco, and D. A. Perez, "A simulation study of the performance of GPC and PID applied to a binary distillation column," in *2021 IEEE International Conference on Automation/24th Congress of the Chilean Association of Automatic Control, ICA-ACCA 2021*, Institute of Electrical and Electronics Engineers Inc., Mar. 2021. doi: 10.1109/ICAACCA51523.2021.9465198.

[6] Chao Ou and Weixing Lin, "Comparison between PSO and GA for Parameters Optimization of PID Controller," in *Proceedings of the 2006 IEEE International Conference on Mechatronics and Automation June 25 - 28, 2006, Luoyang, China*, 2006, pp. 2471–2475.

[7] S. Charkoutsis and M. Kara-Mohamed, "A Particle Swarm Optimization tuned nonlinear PID controller with improved performance and robustness for First Order Plus Time Delay systems," *Results in Control and Optimization*, vol. 12, Sep. 2023, doi: 10.1016/j.rico.2023.100289.

[8] K. Charles, N. Urasaki, T. Senjyu, M. E. Lotfy, and L. Liu, "Robust load frequency control schemes in power system using optimized PID and model predictive controllers," *Energies (Basel)*, vol. 11, no. 11, 2018, doi: 10.3390/en11113070.

[9] Y. S. Cheng, H. Y. Pai, and Y. H. Liu, "PID parameter tuning for flyback converter with synchronous rectification using particle swarm optimization," in *2022 Joint 12th International Conference on Soft Computing and Intelligent Systems and 23rd International Symposium on Advanced Intelligent Systems, SCIS and ISIS 2022*, Institute of Electrical and Electronics Engineers Inc., 2022. doi: 10.1109/SCISISIS55246.2022.10002077.

[10] R. S. Patil, S. P. Jadhav, and M. D. Patil, "Review of Intelligent and Nature-Inspired Algorithms-Based Methods for Tuning PID Controllers in Industrial Applications," Journal of Robotics and Control, vol. 5, no. 2, 2024, doi: 10.18196/jrc.v5i2.20850.

[11] N. Ajlouni, A. Osyavas, F. Ajlouni, A. Almassri, F. Takaoglu, and M. Takaoglu, "Enhancing PID control robustness in CSTRs: a hybrid approach to tuning under external disturbances with GA, PSO, and machine learning," Neural Computing and Applications, vol. 37, pp. 12153–12177, 2025, doi: 10.1007/s00521-025-11170-0.

[12] Z. Hu, W. Guo, K. Zhou, L. Wang, F. Wang, and J. Yuan, "Optimization of PID control parameters for marine dual-fuel engine using improved particle swarm algorithm," Scientific Reports, vol. 14, article 12681, 2024, doi: 10.1038/s41598-024-63253-y.

[13] Y. Yang, Y. Gao, J. Wu, Z. Ding, and S. Zhao, "Improving PID Controller Performance in Nonlinear Oscillatory Automatic Generation Control Systems Using a Multi-objective Marine Predator Algorithm with Enhanced Diversity," Journal of Bionic Engineering, vol. 21, pp. 2497–2514, 2024, doi: 10.1007/s42235-024-00548-w.

[14] N. N. Mohammad *et al.*, "Comparison of the performance and energy consumption between PID control and self-tuning FuzzyPID in compact hydro distillation process," in *Proceedings - 2018 IEEE International Conference on Automatic Control and Intelligent Systems, I2CACIS 2018*, 2019, pp. 7–12. doi: 10.1109/I2CACIS.2018.8603679.

[15] N. Mustafa and F. H. Hashim, "Design of a Predictive PID Controller Using Particle Swarm Optimization," *International Journal of Electronics and Telecommunications*, pp. 737–743, Jul. 2020, doi: 10.24425/ijet.2020.134035.

[16] A. H. A. Nasir, N. Hambali, and M. H. F. Rahiman, "Implementation of PRBS & RGS Perturbation Input Signals on Steam Temperature: Model Estimation and PID Control," in *2023 19th IEEE International Colloquium on Signal Processing and Its Applications, CSPA 2023 - Conference Proceedings*, Institute of Electrical and Electronics Engineers Inc., 2023, pp. 99–104. doi: 10.1109/CSPA57446.2023.10087748.

[17] Nurul Nadia Mohammad, Ahmad Aftas Azman, Mohd Hezri Marzaki, Ramli Adnan, Mazidah Tajjudin, and Mohd Hezri Fazalul Rahiman, "Performance Comparison and Energy Consumption Index Between MPC and FuzzyPID in Small-scaled Agarwood Distillation Pot," in *2018 9th IEEE Control and System Graduate Research Colloquium (ICSGRC 2018), 3 - 4 August 2018, Shah Alam, Malaysia*, 2018, pp. 156–161.

[18] Nurul Nadia Mohammad, Mohd Hezri Marzaki, Ramli Adnan, and Mohd Hezri Fazalul Rahiman, "Evaluation of Energy Consumption in Small-scale Agarwood Distillation Pot based on Averaged Control Signal Simulation," in *2017 IEEE 13th International Colloquium on Signal Processing & its Applications (CSPA 2017), 10 - 12 March 2017, Penang, Malaysia*, 2017, pp. 275–280.

[19] M. Rahimian and K. Raahemifar, "OPTIMAL PID CONTROLLER DESIGN FOR AVR SYSTEM USING PARTICLE SWARM OPTIMIZATION ALGORITHM," 2011.

[20] A. F. dos Santos Neto, B. S. Campelo, M. S. Freitas, M. F. dos Santos, V. B. Schettino, and P. Mercorelli, "Enhancing Performance of Level System Modeling with Pseudo-Random Signals," in *Proceedings of the 2024 25th International Carpathian Control Conference, ICCC 2024*, Institute of Electrical and Electronics Engineers Inc., 2024. doi: 10.1109/ICCC62069.2024.10569309.

[21] Mazidah Tajjudin, M. Azfar Abdullah Pani, Sakinah Abdul Aziz, Norlela Ishak and Ramli Adnan, "A_Study_on_IMC-based_PID_for_Steam_Distillation_Process," in *2018 IEEE International Conference on Automatic Control and Intelligent System (12ACIS 2018), 20 October 2018, Shah Alam, Malaysia*, 2018, pp. 133–136.

[22] C. Lianbo *et al.*, "Parameter Tuning of PID Controller of Servo System Based on Particle Swarm Optimization Algorithm," in *IOP Conference Series: Materials Science and Engineering*, Institute of Physics Publishing, 2019. doi: 10.1088/1757-899X/533/1/012022.

[23] I. A. Abbas and K. Mustafa, "A review of adaptive tuning of PID-controller: Optimization techniques and applications," *Int. J. Nonlinear Anal. Appl*, vol. 15, pp. 2008–6822, 2024, doi: 10.22075/ijnaa.2023.21415.4024.

[24] K. Latha, V. Rajinikanth, and P. M. Surekha, "PSO-Based PID Controller Design for a Class of Stable and Unstable Systems," *ISRN Artificial Intelligence*, vol. 2013, pp. 1–11, May 2013, doi: 10.1155/2013/543607.

[25] R. Singh and L. Ramesh, "Comparison between PID and PSO-PID controllers in analysing the load frequency control in interconnected microgrids in a deregulated environment," *International Journal of Global Energy Issues*, vol. 46, no. 1–2, pp. 112–136, 2023, doi: 10.1504/IJGEI.2024.135249.

[26] F. Pangerang, F. A. Samman, Z. Zainuddin, and R. S. Sadjad, "Variable loaded brushless DC motor with six step commutation PID-based speed controller optimized by PSO algorithm," *Bulletin of Electrical Engineering and Informatics*, vol. 14, no. 1, pp. 132–142, Feb. 2025, doi: 10.11591/eei.v14i1.8618.

[27] S. Ylldlrlm, M. S. Bingol, and S. Savas, "Tuning PID controller parameters of the DC motor with PSO algorithm," *International Review of Applied Sciences and Engineering*, Oct. 2024, doi: 10.1556/1848.2023.00698.

[28] M. Saif, V. Singh, A. Rani, and J. Yadav, "Particle Swarm Optimization based Fractional Order PID Control for the Twin Rotor Multi-Input Multi- Output System," in *2024 3rd International Conference on Power Electronics and IoT Applications in Renewable Energy and its Control, PARC 2024*, Institute of Electrical and Electronics Engineers Inc., 2024, pp. 292–296. doi: 10.1109/PARC59193.2024.10486531.